



Synthesis and characterization of nanosized $Mg_xMn_{1-x}Fe_2O_4$ ferrites by both sol-gel and thermal decomposition methods



Laura Elena De-León-Prado^{a,*}, Dora Alicia Cortés-Hernández^a, José Manuel Almanza-Robles^a, José Concepción Escobedo-Bocardo^a, Javier Sánchez^a, Pamela Yajaira Reyes-Rdz^a, Rosario Argentina Jasso-Terán^a, Gilberto Francisco Hurtado-López^b

^a Cinvestav-Unidad Saltillo, Av. Industria Metalúrgica #1062, Parque Industrial Saltillo-Ramos Arizpe, CP 25900, Ramos Arizpe, Coahuila, México

^b Centro de Investigación en Química Aplicada, Blvd. Enrique Reyna Hermosillo #140, CP 25294, Saltillo, Coahuila, México

ARTICLE INFO

Keywords:

Sol-gel
Thermal decomposition
Magnetic nanoparticles
Superparamagnetism

ABSTRACT

This work reports the synthesis of $Mg_xMn_{1-x}Fe_2O_4$ ($x=0-1$) nanoparticles by both sol-gel and thermal decomposition methods. In order to determine the effect of synthesis conditions on the crystal structure and magnetic properties of the ferrites, the synthesis was carried out varying some parameters, including composition. By both methods it was possible to obtain ferrites having a single crystalline phase with cubic inverse spinel structure and a behavior near to that of superparamagnetic materials. Saturation magnetization values were higher for materials synthesized by sol-gel. Furthermore, in both cases particles have a spherical morphology and nanometric sizes (11–15 nm). Therefore, these materials can be used as thermoseeds for the treatment of cancer by magnetic hyperthermia.

1. Introduction

The rapidly increasing number of people with cancer has led to the development of newer and better treatments for this disease. Among these treatments, magnetic hyperthermia has attracted attention due to the overcome of some of the disadvantages in comparison to the conventional treatments. In general, magnetic hyperthermia takes advantage of the capability of magnetic nanoparticles to produce heat under the action of an external magnetic field. The use of magnetic nanoparticles in biomedical areas has occurred as a result of the numerous benefits that provide their large surface area, dimension similar or even lower than cells and also the possibility that these particles offer to be coated for their interaction with the biological medium [1,2]. For this reason, the development of new materials as well as new synthesis methods is an important field of research nowadays. Among the different materials for hyperthermia applications, iron oxides such as magnetite and maghemite, are the more used [2–4]. Ferrites can be obtained by different methods and they can be classified into three different crystal systems (spinel, garnets and hexaferrites) [5]. Cubic spinel ferrites have the general formula MFe_2O_4 , where oxygen forms an fcc close packing, and Fe^{3+} and M^{2+} occupy either tetrahedral or octahedral interstitial sites [6], M is a divalent metallic ion such as Fe^{2+} , Ni^{2+} , Cu^{2+} , Mg^{2+} , Mn^{2+} , Zn^{2+} , or a

mixture of them [7]. Some of the methods for synthesizing nanometric ferrites include coprecipitation, citrate precursor, reverse micelle, sol-gel, thermal decomposition, etc. [5]. Sol-gel method offers some advantages that include high purity, good homogeneity and low cost, and the thermal decomposition method allows obtaining mixed ferrites from the decomposition of metal acetylacetonates in an organic phase at relatively low temperatures [8–10]. In addition, by thermal decomposition methods nanoparticles with smaller sizes are obtained in comparison to those obtained by sol-gel [6]. However, by sol-gel method a higher crystallinity of nanoparticles has been observed [8]. Furthermore the chemically stable structures that ferrites have, these type of materials offer the possibility of being molecularly engineered to provide a wide range of magnetic properties by adjusting the chemical composition of M^{2+} [6,11]. Hence, this work reports the synthesis of $Mg_xMn_{1-x}Fe_2O_4$ ($x=0-1$) nanoparticles by both sol-gel and thermal decomposition methods. Synthesis was carried out varying the heat treatment temperature and crystallization time for sol-gel method and time of reaction for thermal decomposition method. This in order to additionally determine the effect of heat treatment temperature and time on the crystal structure and magnetic properties of the nanoparticles.

* Corresponding author.

E-mail addresses: laura.elena.prado@gmail.com, laura_prado7@hotmail.com (L.E. De-León-Prado).

2. Materials and methods

For the sol-gel route, stoichiometric amounts of $\text{Fe}(\text{NO}_3)_3 \cdot 9\text{H}_2\text{O}$, $\text{Mg}(\text{NO}_3)_2 \cdot 6\text{H}_2\text{O}$ and $\text{Mn}(\text{NO}_3)_2 \cdot 4\text{H}_2\text{O}$ were dissolved into 5 mL of $\text{C}_2\text{H}_6\text{O}_2$ in a 100 mL beaker. This solution was stirred for 2 h at 40 °C, and then the obtained sol was heated up to 80 °C and kept at this temperature until a brown gel was formed. The gel was aged for 2 h at room temperature and then dried at 95 °C for 72 h. Subsequently, the dried gel was heat treated at 400, 500 or 600 °C in air for 30, 60, 90 or 120 min. The obtained products were milled and then washed several times with ethanol, in order to remove the ethylene glycol excess. Finally, the powders were dried at room temperature. For the thermal decomposition method, stoichiometric amounts of the acetylacetonates of Fe, Mg and Mn, phenyl ether and oleic acid were placed in a three-necked flask of 250 mL. Subsequently, a thermometer was placed in one of the side necks and a reflux system was adapted. The solution was heated up to 250 °C and it was maintained at this temperature for 30, 60 or 90 min. Once the reaction time passed, a precipitate was obtained, which was washed repeatedly with ethanol. Finally, the precipitate was dried at room temperature and milled. The characterization of the products was carried out by X-ray diffraction (XRD), vibrating sample magnetometry (VSM) and transmission electron microscopy (TEM).

3. Results and discussion

Fig. 1 shows the XRD patterns (a,b) of $\text{Mg}_x\text{Mn}_{1-x}\text{Fe}_2\text{O}_4$ ($x=0-1$) nanoparticles synthesized by both sol-gel (heat treatment temperature of 500 °C and crystallization time of 60 min) and thermal decomposition (time of reaction 60 min) methods. The reflections correspond to those of ferrites with a cubic inverse spinel structure, and are similar to those of MgFe_2O_4 (JCPDS 88-1935). Furthermore, it is possible to observe, for both methods that as the concentration of Mn increases, there is a slight shift of the reflections to higher angles, which can be attributed to the incorporation of a cation with greater radius (Mn), compared with the ionic radii of Fe and Mg, into the crystalline structure. The hysteresis loops of the selected ferrites for both methods, as well as MnFe_2O_4 and MgFe_2O_4 , are shown in Fig. 1(c and d). These

materials have a soft ferrimagnetic behavior close to superparamagnetic materials as the typical sigmoidal curve shape occurs.

Table 1 shows the magnetic properties and crystallite size (calculated using the Scherrer equation) of $\text{Mg}_x\text{Mn}_{1-x}\text{Fe}_2\text{O}_4$ ($x=0-1$) synthesized by both sol-gel (heat treatment temperature of 500 °C and crystallization time of 60 min) and thermal decomposition (time of reaction 60 min). These results show for the case of sol-gel method, that the values of saturation magnetization (M_s) increase gradually as the concentration of Mn is increased, ranging from 25.58 to 48.73 emu/g. The corresponding values for remanent magnetization (M_r) and coercivity (H_c) vary between 0 and 1.75 emu/g, and 0 and 50 Oe, respectively. For the case of thermal decomposition method, an opposite tendency was observed, the values of M_s decrease gradually as the concentration of Mn cations is increased, ranging from 10.86 to 35.16 emu/g. The corresponding values of M_r and H_c in this case have a variation between 0 and 1.72 emu/g, and 0 and 70 Oe, respectively.

Taking into account that the net magnetic moment is given by the difference between the magnetic moments of the octahedral sites and tetrahedral sites (total net $\mu_B = \mu_B(\text{octahedral-site}) - \mu_B(\text{tetrahedral-site})$) [11], it can be noticed that the cations distribution in the interstitial sites of the spinel structure has a major influence on the values of M_s . This distribution of cations is also influenced by other factors, which include the ionic radius, oxidation state, atomic diameter, exchange and superexchange interactions, etc. [12,13]; and some of these factors also depend on specific parameters of the synthesis method, such as temperature and reaction atmosphere. In this case, the main factor for controlling the distribution of cations during the two methods used is temperature. This due to the fact that temperature is able to change the oxidation state of cations and thus their redistribution. When Mn cations ($\mu_B=5$) occupy octahedral sites, replacing Fe cations ($\mu_B=5$), there is not a change in the magnetic moment; and when Mg cations ($\mu_B=0$) occupy tetrahedral sites, replacing Fe cations ($\mu_B=5$), the magnetic moment decreases. This change results in an increase of the net magnetic moment and therefore in the value of M_s . At the heat treatment temperatures used in sol-gel method (400, 500 and 600 °C) the Mn cations are more probably to be present in the oxidation state Mn^{3+} . In this state the ionic radius is smaller than that of Mn^{2+} and could favor a higher degree of occupancy of these cations, over Mg

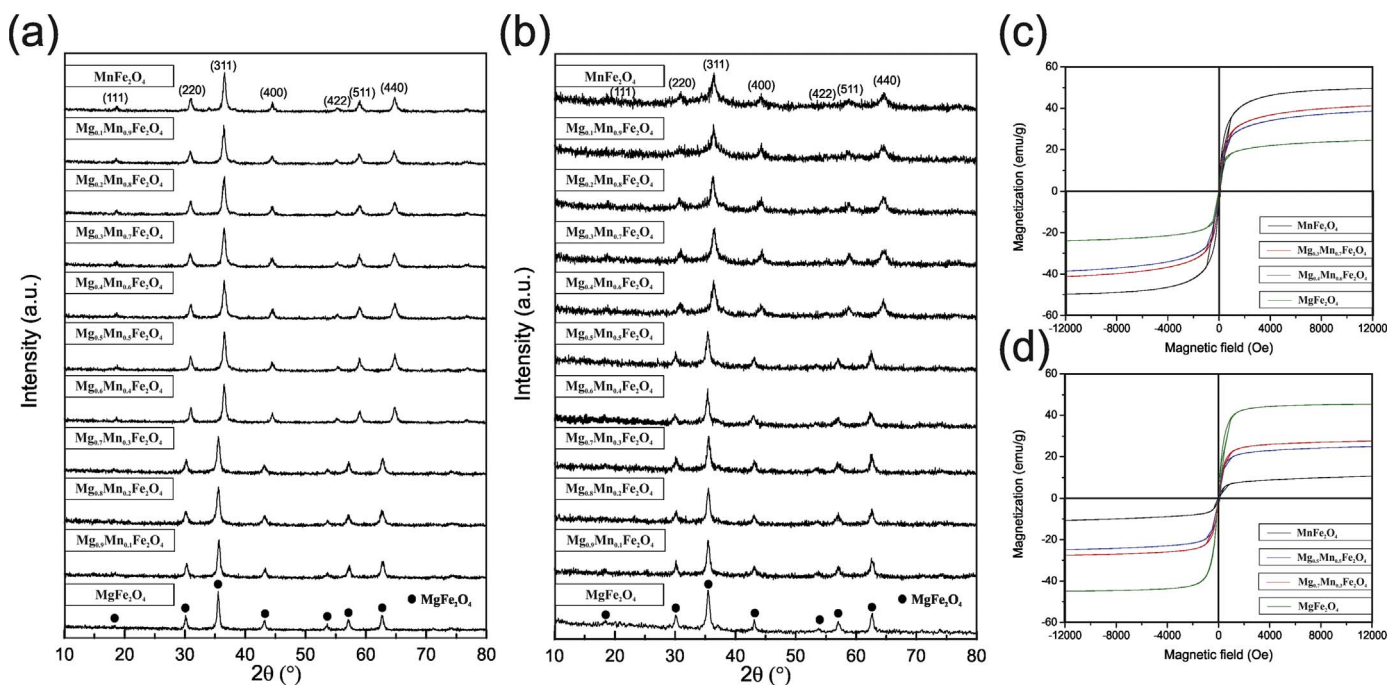


Fig. 1. XRD patterns and hysteresis loops of $\text{Mg}_x\text{Mn}_{1-x}\text{Fe}_2\text{O}_4$ nanoparticles synthesized by (a,c) sol-gel method and (b,d) thermal decomposition method.

Table 1

Magnetic properties and crystallite sizes of $\text{Mg}_x\text{Mn}_{1-x}\text{Fe}_2\text{O}_4$ ($x=0-1$) nanoparticles synthesized by sol-gel (heat treated at 500 °C for 60 min) and thermal decomposition (reaction time of 60 min) methods.

$\text{Mg}_x\text{Mn}_{1-x}\text{Fe}_2\text{O}_4$ ($x=0-1$)	Saturation M_s (emu/g)		Remanence M_r (emu/g)		Coercivity H_c (Oe)		Crystallite size (nm)	
	Sol-gel	Thermal decomposition	Sol-gel	Thermal decomposition	Sol-gel	Thermal decomposition	Sol-gel	Thermal decomposition
MnFe_2O_4	49.71	10.69	1.01	0.66	10	50	18	8
$\text{Mg}_{0.1}\text{Mn}_{0.9}\text{Fe}_2\text{O}_4$	48.73	10.86	0.93	0.11	13	9	17	14
$\text{Mg}_{0.2}\text{Mn}_{0.8}\text{Fe}_2\text{O}_4$	43.94	15.48	1.75	0.28	40	18	15	9
$\text{Mg}_{0.3}\text{Mn}_{0.7}\text{Fe}_2\text{O}_4$	41.25	17.85	0.78	1.72	10	70	15	10
$\text{Mg}_{0.4}\text{Mn}_{0.6}\text{Fe}_2\text{O}_4$	38.65	19.82	0	1.04	0	21	15	8
$\text{Mg}_{0.5}\text{Mn}_{0.5}\text{Fe}_2\text{O}_4$	34.91	24.94	1.04	0	23	0	14	11
$\text{Mg}_{0.6}\text{Mn}_{0.4}\text{Fe}_2\text{O}_4$	34.39	22.54	0.33	0.52	50	12	19	15
$\text{Mg}_{0.7}\text{Mn}_{0.3}\text{Fe}_2\text{O}_4$	30.41	27.60	1.57	0.50	25	8	16	14
$\text{Mg}_{0.8}\text{Mn}_{0.2}\text{Fe}_2\text{O}_4$	28.07	28.78	0.29	1.04	15	28	14	9
$\text{Mg}_{0.9}\text{Mn}_{0.1}\text{Fe}_2\text{O}_4$	25.58	35.16	0.36	1.68	6	18	16	15
MgFe_2O_4	24.30	45.20	0.56	0	10	0	21	17

cations, in the octahedral sites of the structure, increasing the net magnetic moment and therefore the M_s . This occupancy is also favored by the concentration of the cations; as the concentration of Mn is increased, it is expected that more sites are occupied by these cations and therefore the value of M_s increases. Contrary to this, in thermal decomposition method, the oxidation of Mn^{2+} to Mn^{3+} is not promoted by the temperature of 250 °C, as in sol-gel method, and in consequence the occupancy of these cations in the octahedral sites is decreased. The occupancy of Mn cations in tetrahedral sites results in a decrease of the net magnetic moment, and therefore in M_s . This also is influenced by concentration, and it is expected that as the content of Mn cations decreases, the degree of occupancy of these cations in tetrahedral sites also decreases, and in consequence the value of M_s is increased.

The M_s value is influenced only by the composition of materials; however, H_c is more influenced by the structure, which causes it to have different values depending on the defects of the material. This can be seen in the results obtained for both methods, in which there is not a tendency of the data. A low value of H_c indicates that the domain walls can be easily moved when an applied magnetic field changes in magnitude or direction; however, when there are non-magnetic

particles or voids in the materials, the domain walls are restricted in their movement and the values of H_c increase [14].

The use of magnetic nanoparticles for applications such as magnetic hyperthermia is restricted by the values of M_s , M_r and H_c . The reason of this lays on the behavior of the nanoparticles once they are introduced into the living tissues. A high value of M_s is required due to the fact that it is directly related to obtaining a high degree of heating capability of the particles and therefore to the use of a low concentration of the particles to achieve a desired temperature. Values close to zero of M_r and H_c are required for obtaining nanoparticles with a behavior very similar to that of superparamagnetic materials. Particles having this behavior are going to show magnetic properties only in the presence of an external magnetic field and therefore the risk of physiological effects, such as an alteration in the homeostasis of the living medium or the formation of clots that may provoke an embolism, is reduced. Therefore, the ferrites that presented the best relationship between these parameters were $\text{Mg}_{0.3}\text{Mn}_{0.7}\text{Fe}_2\text{O}_4$ and $\text{Mg}_{0.4}\text{Mn}_{0.6}\text{Fe}_2\text{O}_4$ synthesized by sol-gel method, and $\text{Mg}_{0.5}\text{Mn}_{0.5}\text{Fe}_2\text{O}_4$ and $\text{Mg}_{0.7}\text{Mn}_{0.3}\text{Fe}_2\text{O}_4$ synthesized by thermal decomposition method.

Fig. 2 shows the XRD patterns (a,b) and hysteresis loops (c,d) of the

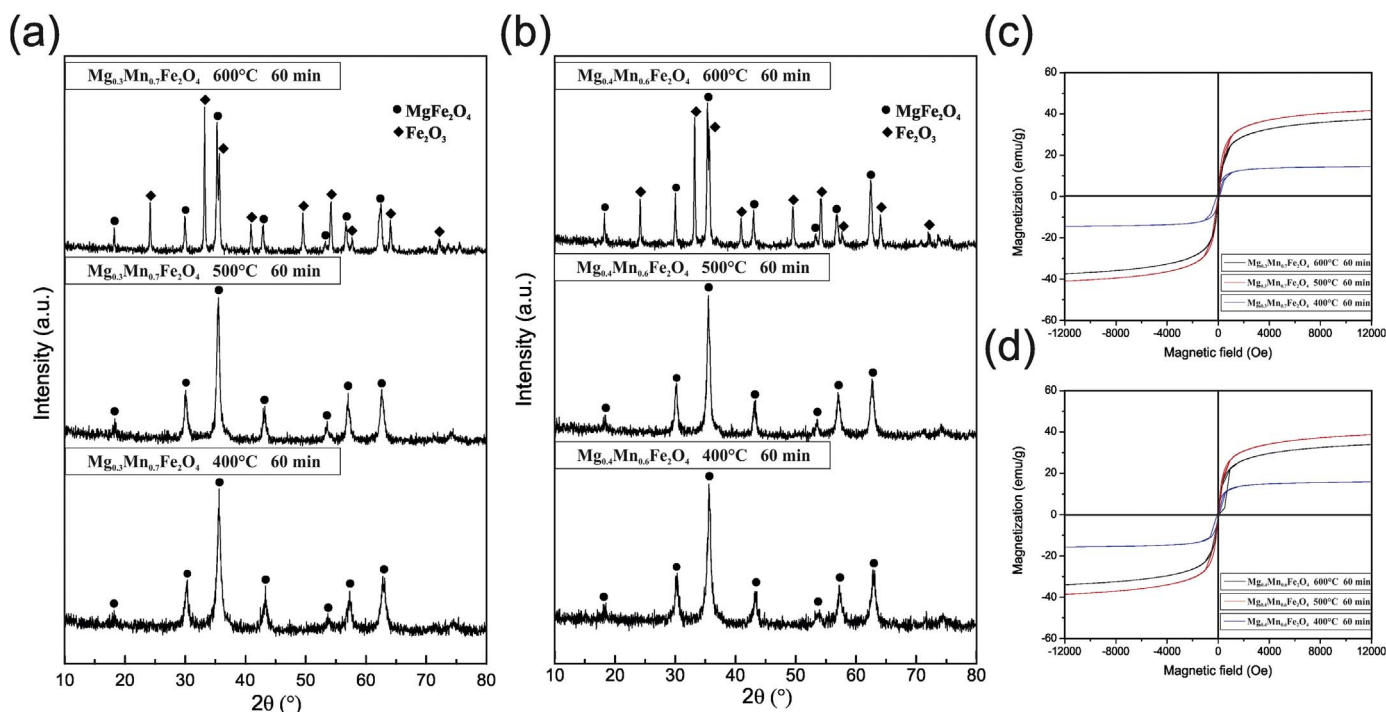


Fig. 2. XRD patterns and hysteresis loops of $\text{Mg}_x\text{Mn}_{1-x}\text{Fe}_2\text{O}_4$ nanoparticles synthesized by sol-gel method (a,c) $x=0.3$ and (b,d) $x=0.4$.

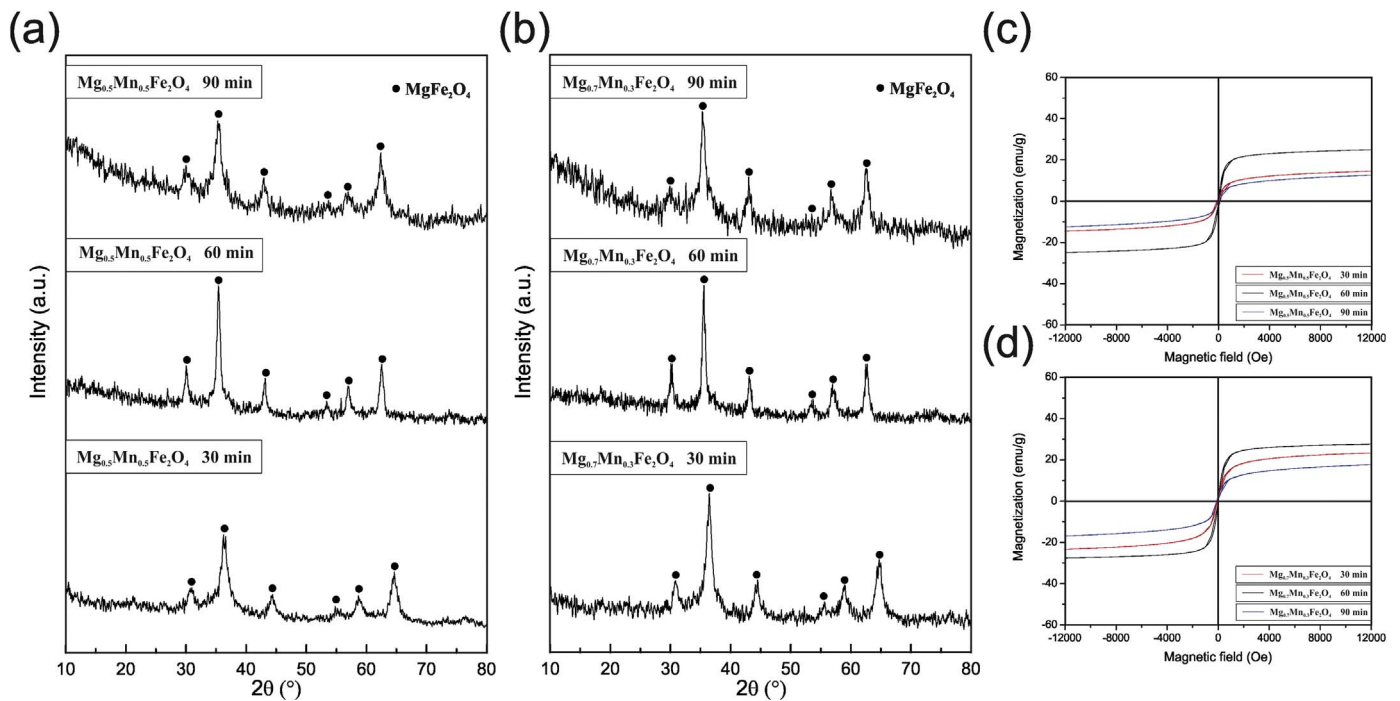


Fig. 3. XRD patterns and hysteresis loops of $Mg_xMn_{1-x}Fe_2O_4$ synthesized by thermal decomposition method (a,c) $x=0.5$ and (b,d) $x=0.7$.

selected ferrites synthesized by sol-gel method. For both ferrites, at the heat treatment temperature of 600 °C, occurs the formation of a secondary phase, which was identified as hematite (JCPDS 33-0664). This phase is undesirable and thus the materials treated at 600 °C were no longer considered. In accordance to the hysteresis loops (Fig. 2(c and d)), the most suitable magnetic properties were obtained at 500 °C, hence this temperature was used to evaluate the effect of crystallization time.

Fig. 3 shows the XRD patterns (a,b) and hysteresis loops (c,d) of $Mg_{0.5}Mn_{0.5}Fe_2O_4$ and $Mg_{0.7}Mn_{0.3}Fe_2O_4$ synthesized by thermal de-

composition method with times of reaction of 30, 60 or 90 min. For both ferrites, there is no formation of secondary phases. Accordingly to the hysteresis loops, the most suitable magnetic properties were obtained at the reaction time of 60 min, therefore this reaction time was selected for further investigation.

Fig. 4 shows the XRD patterns (a,b) and hysteresis loops (c,d) of $Mg_{0.3}Mn_{0.7}Fe_2O_4$ and $Mg_{0.4}Mn_{0.6}Fe_2O_4$ synthesized by sol-gel method, heat treated at 500 °C with crystallization times of 30, 60, 90 or 120 min. In both ferrites, there is no formation of secondary phases. In accordance to the hysteresis loops, the most suitable magnetic proper-

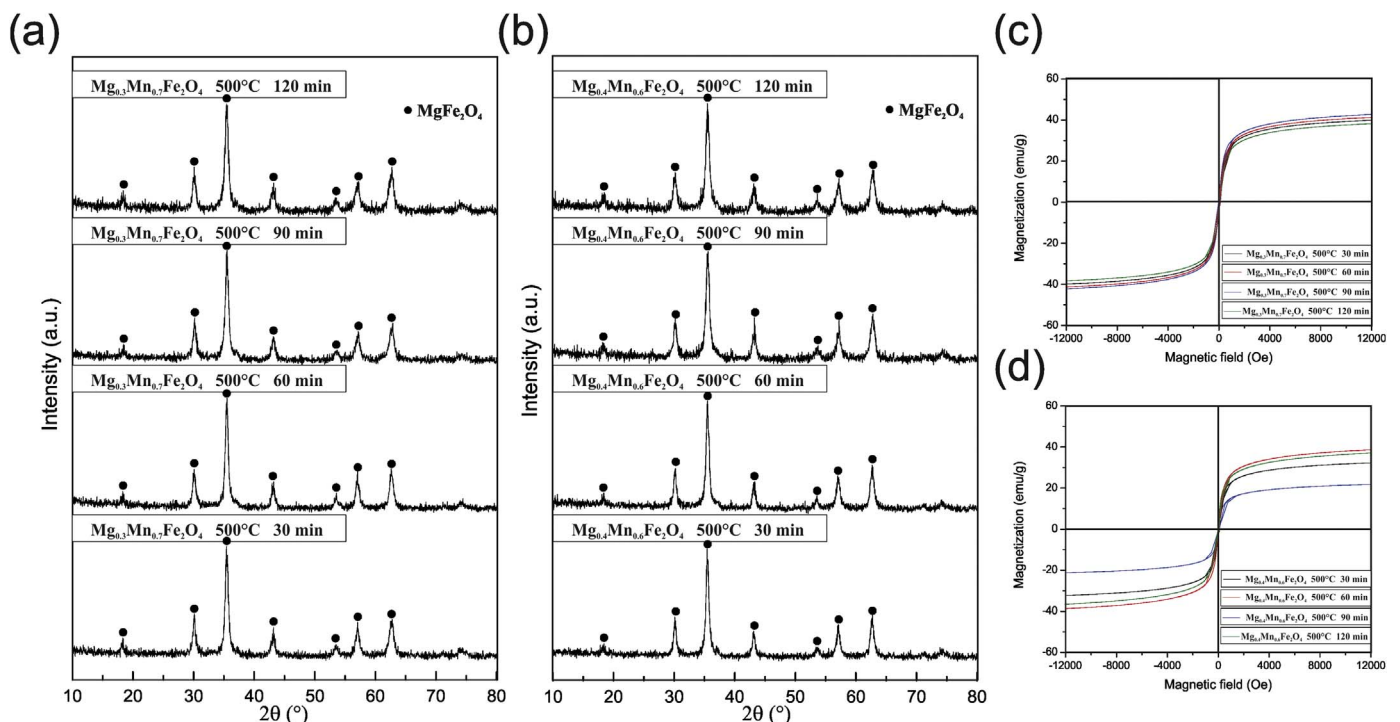


Fig. 4. XRD patterns and hysteresis loops of $Mg_xMn_{1-x}Fe_2O_4$ synthesized by sol-gel method (a,c) $x=0.3$ and (b,d) $x=0.4$.

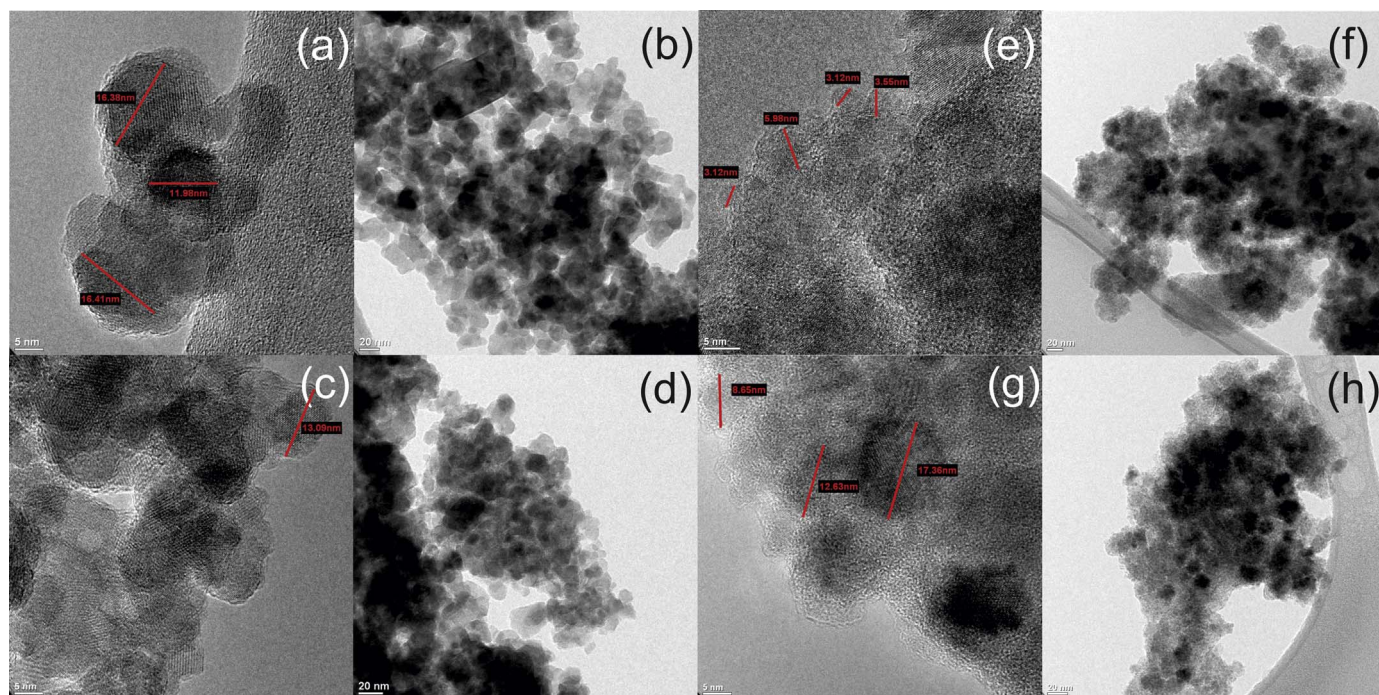


Fig. 5. TEM images of (a,b) $\text{Mg}_{0.3}\text{Mn}_{0.7}\text{Fe}_2\text{O}_4$ and (c,d) $\text{Mg}_{0.4}\text{Mn}_{0.6}\text{Fe}_2\text{O}_4$ nanoparticles synthesized by sol-gel method (heat treated at 500 °C for 60 min), and (e,f) $\text{Mg}_{0.5}\text{Mn}_{0.5}\text{Fe}_2\text{O}_4$ and (g,h) $\text{Mg}_{0.7}\text{Mn}_{0.3}\text{Fe}_2\text{O}_4$ nanoparticles synthesized by thermal decomposition method (reaction time of 60 min).

ties were obtained at the crystallization time of 60 min.

Fig. 5 shows TEM images of the selected ferrites, $\text{Mg}_{0.3}\text{Mn}_{0.7}\text{Fe}_2\text{O}_4$ (a,b) and $\text{Mg}_{0.4}\text{Mn}_{0.6}\text{Fe}_2\text{O}_4$ (c,d) synthesized by sol-gel and $\text{Mg}_{0.5}\text{Mn}_{0.5}\text{Fe}_2\text{O}_4$ (e,f) and $\text{Mg}_{0.7}\text{Mn}_{0.3}\text{Fe}_2\text{O}_4$ (g,h) synthesized by thermal decomposition method. As observed for all ferrites, particles have a spherical-like morphology and sizes in accordance to those calculated (Scherrer equation). Additionally, agglomerates can be observed, this due to the soft ferrimagnetic behavior (near to the superparamagnetic regime) that the materials show according to the hysteresis loops. Iftikhar et al. [15], also reported that small particles with single domains, experience permanent magnetic moments and therefore each particle is permanently magnetized and tend to agglomerate. Furthermore, it is well known that nanosized particles (even no magnetic ones) tend to agglomerate due to Van der Waals forces and high surface energy [16].

4. Conclusions

Nanometric Mg-Mn ferrites were successfully synthesized by both sol-gel and thermal decomposition methods. In all the cases, a single cubic inverse spinel crystalline structure and a nearly superparamagnetic behavior were observed. In addition, the ferrites composition and the synthesis method have an effect on the magnetic properties; this probably due to the differences in the incorporation of metal ions into the structure of the spinel. Higher values of saturation magnetization were obtained for the materials synthesized by sol-gel and thermal decomposition method. The ferrites $\text{Mg}_{0.3}\text{Mn}_{0.7}\text{Fe}_2\text{O}_4$ and $\text{Mg}_{0.4}\text{Mn}_{0.6}\text{Fe}_2\text{O}_4$ synthesized by sol-gel (with a heat treatment temperature of 500 °C and crystallization time of 60 min), and the ferrites $\text{Mg}_{0.5}\text{Mn}_{0.5}\text{Fe}_2\text{O}_4$ and $\text{Mg}_{0.7}\text{Mn}_{0.3}\text{Fe}_2\text{O}_4$ synthesized by thermal decomposition (with a time of reaction of 60 min), showed a spherical-like morphology and nanometric sizes (11–15 nm). Therefore, these nanoparticles can be used as thermoseeds for the treatment of cancer by magnetic hyperthermia.

References

- [1] C.C. Berry, A.S.G. Curtis, Functionalisation of magnetic nanoparticles for applications in biomedicine, *J. Phys. Appl. Phys.* 36 (2003) R198.
- [2] Q.A. Pankhurst, J. Connolly, S.K. Jones, J. Dobson, Applications of magnetic nanoparticles in biomedicine, *J. Phys. Appl. Phys.* 36 (2003) R167.
- [3] B. Thiesen, A. Jordan, Clinical applications of magnetic nanoparticles for hyperthermia, *Int. J. Hyperthermia* 24 (2008) 467–474.
- [4] V.I. Shubayev II, T. R. P. S. Jin, Magnetic nanoparticles for theragnostics, *Adv. Drug Deliv. Rev.* 61 (2009) 467–477.
- [5] R. Valenzuela, Novel applications of ferrites, *Phys. Res. Int.* 2012 (2012).
- [6] Shouheng Sun, et al., Monodisperse MFe_2O_4 (M=Fe, Co, Mn) nanoparticles, *J. Am. Chem. Soc.* 126 (2004) 273–279.
- [7] M.M. Hessien, M.M. Rashad, K. El-Barawy, I.A. Ibrahim, Influence of manganese substitution and annealing temperature on the formation, microstructure and magnetic properties of Mn–Zn ferrites, *J. Magn. Magn. Mater.* 320 (2008) 1615–1621.
- [8] A.M. Escamilla-Pérez, D.A. Cortés-Hernández, J.M. Almanza-Robles, D. Mantovani, P. Chevallier, Crystal structure of superparamagnetic $\text{Mg}_{0.2}\text{Ca}_{0.8}\text{Fe}_2\text{O}_4$ nanoparticles synthesized by sol-gel method, *J. Magn. Magn. Mater.* 374 (2015) 474–478.
- [9] J. Aswathy, M. Suresh, Ferrofluids: synthetic strategies, stabilization, physico-chemical features, characterization, and applications, *ChemPlusChem* 79 (2014) 1382–1420.
- [10] R. Betancourt-Galindo, et al., Synthesis of copper nanoparticles by thermal decomposition and their antimicrobial properties, *J. Nanomater.* 2014 (2014) 10:10–10:10.
- [11] M. Jeun, et al., Physical parameters to enhance AC magnetically induced heating power of ferrite nanoparticles for hyperthermia in nanomedicine, *IEEE Trans. Nanotechnol.* 12 (2013) 314–322.
- [12] I. Nebot Díaz, Estudio y caracterización de compuestos tipo espinela $\text{M}^{\text{II}}\text{Al}_2\text{O}_4$, mediante rutas de síntesis no convencionales. Aplicación a la industria cerámica. Universitat Jaume I. Departament de Química Inorgànica i Orgànica; Carda Castelló, Juan B., 2001.
- [13] E. Pollert, Crystal chemistry of magnetic oxides part 1: General problems – Spinel, *Prog. Cryst. Growth Charact.* 9 (1984) 263–323.
- [14] W.D. Callister (Ed.) *Materials Science and Engineering: An Introduction*, John Wiley & Sons, Inc., USA, 2007, pp. 76–109.
- [15] A. Iftikhar, et al., Synthesis of super paramagnetic particles of $\text{Mn}_{1-x}\text{Mg}_x\text{Fe}_2\text{O}_4$ ferrites for hyperthermia applications, *J. Alloy. Compd.* 601 (2014) 116–119.
- [16] A.K. Gupta, M. Gupta, Synthesis and surface engineering of iron oxide nanoparticles for biomedical applications, *Biomaterials* 26 (2005) 3995–4021.